



**HAL**  
open science

## Impurity-limited mobility and variability in gate-all-around silicon nanowires

Y.M. Niquet, H. Mera, C. Delerue

► **To cite this version:**

Y.M. Niquet, H. Mera, C. Delerue. Impurity-limited mobility and variability in gate-all-around silicon nanowires. *Applied Physics Letters*, 2012, 100, pp.153119-1-4. 10.1063/1.4704174 . hal-00787840

**HAL Id: hal-00787840**

**<https://hal.science/hal-00787840>**

Submitted on 27 May 2022

**HAL** is a multi-disciplinary open access archive for the deposit and dissemination of scientific research documents, whether they are published or not. The documents may come from teaching and research institutions in France or abroad, or from public or private research centers.

L'archive ouverte pluridisciplinaire **HAL**, est destinée au dépôt et à la diffusion de documents scientifiques de niveau recherche, publiés ou non, émanant des établissements d'enseignement et de recherche français ou étrangers, des laboratoires publics ou privés.

# Impurity-limited mobility and variability in gate-all-around silicon nanowires

Cite as: Appl. Phys. Lett. **100**, 153119 (2012); <https://doi.org/10.1063/1.4704174>

Submitted: 07 December 2011 • Accepted: 02 April 2012 • Published Online: 13 April 2012

Yann-Michel Niquet, Hector Mera and Christophe Delerue



View Online



Export Citation

## ARTICLES YOU MAY BE INTERESTED IN

[Enhanced impurity-limited mobility in ultra-scaled Si nanowire junctionless field-effect transistors](#)

Applied Physics Letters **107**, 253501 (2015); <https://doi.org/10.1063/1.4937901>

[Nanoscale magnetic field mapping with a single spin scanning probe magnetometer](#)

Applied Physics Letters **100**, 153118 (2012); <https://doi.org/10.1063/1.3703128>

[Modeling of electron mobility in gated silicon nanowires at room temperature: Surface roughness scattering, dielectric screening, and band nonparabolicity](#)

Journal of Applied Physics **102**, 083715 (2007); <https://doi.org/10.1063/1.2802586>

Lock-in Amplifiers  
up to 600 MHz



Zurich  
Instruments



# Impurity-limited mobility and variability in gate-all-around silicon nanowires

Yann-Michel Niquet,<sup>1,a)</sup> Hector Mera,<sup>1,2</sup> and Christophe Delerue<sup>3</sup>

<sup>1</sup>*L. Sim, SP2M, UMR-E CEA/UJF-Grenoble 1, INAC, Grenoble, France*

<sup>2</sup>*IM2NP, UMR CNRS 6242, Marseille, France*

<sup>3</sup>*IEMN - Department ISEN, UMR CNRS 8520, Lille, France*

(Received 7 December 2011; accepted 2 April 2012; published online 13 April 2012)

We discuss the scattering of electrons and holes by charged dopant impurities in  $\langle 001 \rangle$ ,  $\langle 110 \rangle$ , and  $\langle 111 \rangle$  gate-all-around silicon nanowires (Si NWs) with diameters in the 2-8 nm range. We show that the mobility of minority carriers follows simple trends resulting from band-structure effects. In the inversion mode, the  $\langle 110 \rangle$  and  $\langle 001 \rangle$  [respectively,  $\langle 111 \rangle$  and  $\langle 110 \rangle$ ] Si NWs are the best  $n$ -type [resp.  $p$ -type] channels. The choice of a high- $\kappa$  gate oxide is critical to achieve large mobilities in ultimate Si NWs. The mobility of majority carriers is found to increase with decreasing NW diameter and is more weakly dependent on the orientation. We also discuss the variability of single impurity resistances as a function of the structural parameters and nature of the carriers. © 2012 American Institute of Physics. [<http://dx.doi.org/10.1063/1.4704174>]

Silicon nanowires (Si NWs, either etched or grown) have attracted much interest as promising building blocks for ultimate microelectronics devices. In particular, gate-all-around Si NWs transistors shall show improved gate control, hence reduced short-channel effects.<sup>1</sup> Si NWs with diameters below 10 nm have now been synthesized and electrically characterized.<sup>2–7</sup> The data on such small NWs are, however, still scattered and not well understood. It is notably difficult to disentangle the effects of different scattering mechanisms, in a range of dimensions where quantum confinement shapes the electronic structure of the materials. This calls for quantum-mechanical simulations able to sort out the physics of the devices.<sup>8–21</sup>

The need for quantum-mechanical atomistic modeling is particularly evident for impurity scattering. Previous studies have indeed pointed out the limitations of semi-classical approximations,<sup>20</sup> as the current through an impurity may involve a tunneling component or display Fano resonances.<sup>16</sup> However, quantum Green's functions calculations have been mostly limited to very small NWs, with no systematic exploration of the dependence of the transport properties on size and orientation.<sup>15–19,21</sup> In Ref. 20, we have investigated the mobilities of electrons in P and B doped gate-all-around  $\langle 110 \rangle$  Si NWs within an atomistic Green's functions framework. In this letter, we elaborate on this work and discuss the scattering of electrons and holes by charged dopant impurities in  $\langle 001 \rangle$ ,  $\langle 110 \rangle$ , and  $\langle 111 \rangle$  Si NWs with different gate oxides. We give quantitative trends for the mobility of minority and majority carriers, and for the variability of single impurity resistances in the whole  $d = 2\text{--}8$  nm diameter range. We discuss the physics behind these trends and the implications for the design of ultimate devices.

We consider cylindrical Si NWs in a gate-all-around geometry with a 2 nm thick SiO<sub>2</sub> or HfO<sub>2</sub> gate oxide. The electronic structure of the NWs is computed with a  $sp^3d^5s^*$  tight-binding model<sup>22</sup> which is accurate down to the smallest NWs (Ref. 23) and treats all conduction band valleys of sili-

con at once, hence allowing for inter-valleys scattering. The potential of single, charged impurities (P or B) randomly distributed in the cross section of the NW is first calculated using semi-analytical Fourier-Bessel series.<sup>24</sup> This potential is further screened by the free carriers in the conduction or valence band of the NWs within a self-consistent linear response approximation.<sup>20</sup> The impurity-limited mobility  $\mu_{\text{imp}}$  is then calculated from the spatial average  $\langle R_{\text{imp}} \rangle$  of the resistances of at least 16 impurities as

$$\mu_{\text{imp}} = \frac{1}{en_{\text{imp}}nS^2\langle R_{\text{imp}} \rangle}, \quad (1)$$

where  $n_{\text{imp}}$  is the impurity concentration (per unit volume),  $n$  is the free carrier density,  $e$  is the elementary charge, and  $S = \pi d^2/4$  is the cross-sectional area of the NW. The resistance of each individual impurity is obtained with the Landauer-Büttiker formula,<sup>25,26</sup> using a “knitting” algorithm<sup>27</sup> to compute the Green's function and transmission through the NW. Details can be found in Ref. 20. Equation (1) neglects coherent multiple scattering by more than one impurity and is therefore valid only at low  $n_{\text{imp}}$  or in the presence of strong enough inelastic scattering (see discussion at the end of the letter). The data presented in this paper have been computed at room-temperature<sup>28</sup> and for  $n_{\text{imp}} = n = 10^{18} \text{ cm}^{-3}$ .

We first discuss NWs in the inversion regime (transport of “minority” carriers, i.e., electrons in B-doped and holes in P-doped NWs). As discussed in Refs. 16 and 20, charged impurities appear as tunnel barriers for minority carriers and can therefore strongly hinder their flow. The mobility of electrons in B-doped NWs is plotted as a function of diameter in Fig. 1(a), for the three NW orientations and for both SiO<sub>2</sub> and HfO<sub>2</sub> gate oxides. The mobility of holes in P-doped NWs is likewise shown in Fig. 1(b). These figures clearly emphasize (i) the importance of NW orientation and (ii) the need for high- $\kappa$  oxides in ultimate devices to limit charged impurity scattering.

As to electrons, the  $\langle 110 \rangle$ , then  $\langle 001 \rangle$  Si NWs (above  $d = 5$  nm) show the best intrinsic mobilities, while the  $\langle 111 \rangle$

<sup>a)</sup>Electronic mail: yniket@cea.fr.

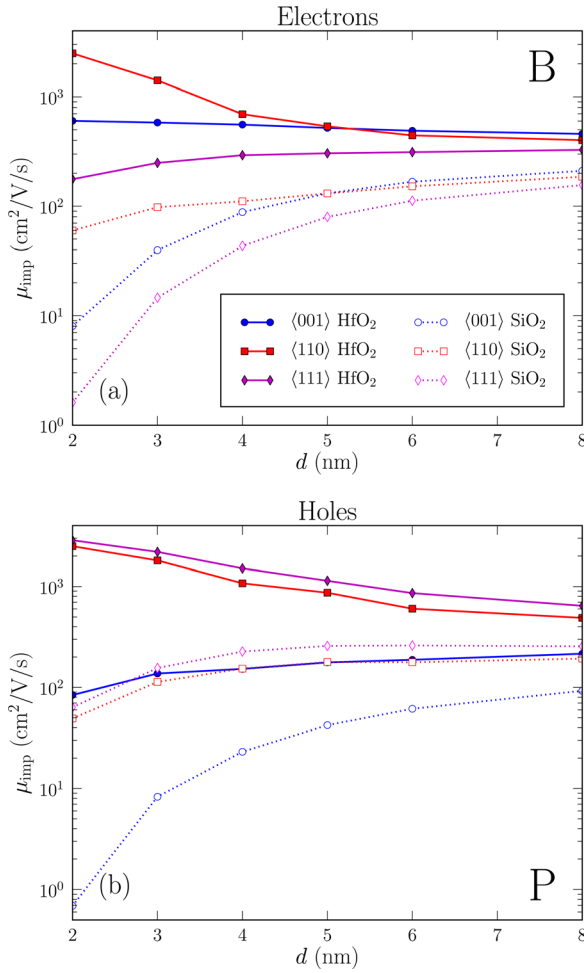


FIG. 1. Impurity-limited mobility of (a) electrons in B doped Si NWs and (b) holes in P doped Si NWs, as a function of diameter  $d$ , for different orientations. The NWs are surrounded by a 2 nm thick HfO<sub>2</sub> or SiO<sub>2</sub> oxide and a metallic gate (gate-all-around geometry). The carrier density and impurity concentrations are  $n = n_{\text{imp}} = 10^{18} \text{ cm}^{-3}$ .

Si NWs perform significantly worse. This strong orientational dependence results from the anisotropy of the band structure of silicon.<sup>29</sup> The confinement indeed lifts the degeneracy between the six conduction band valleys of silicon. The low-energy valleys are only twofold degenerate in  $\langle 110 \rangle$  Si NWs and feature a low effective mass  $m^*$  ranging from  $\lesssim 0.13m_0$  for  $d < 3$  nm to  $m_t^* = 0.19m_0$  for large  $d$ 's. This increases the carrier velocity and limits inter-valleys scattering, thereby enhancing the mobility. The situation is less favorable in small  $\langle 001 \rangle$  Si NWs (fourfold degenerate low-energy valleys with  $m^*$  ranging from  $\gtrsim 0.3m_0$  for  $d < 3$  nm to  $m_t^*$  for large  $d$ 's), and in  $\langle 111 \rangle$  Si NWs (sixfold degenerate valleys with  $m^*$  ranging from  $\gtrsim 1m_0$  for  $d < 3$  nm to  $0.43m_0$  for large  $d$ 's). The spread between the different orientations however decreases with increasing  $d$  as the transport becomes markedly multi-subband. As for holes, the  $\langle 111 \rangle$  and  $\langle 110 \rangle$  Si NWs show the best intrinsic mobilities. Indeed, the lateral confinement tends to promote a non-degenerate light-hole band in these orientations. The effective mass of the holes can actually be as low as  $\simeq 0.13m_0$  in  $\langle 111 \rangle$  Si NWs and  $\simeq 0.18m_0$  in  $\langle 110 \rangle$  Si NWs, while the splitting between the two topmost valence bands is, respectively, 60 and 37 meV at  $d = 3$  nm. These trends in the band

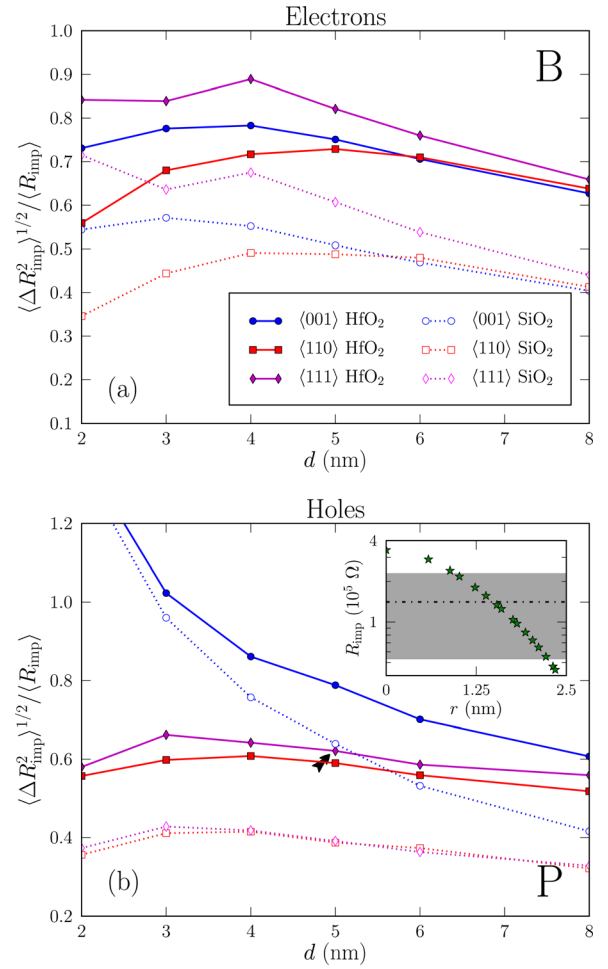


FIG. 2. Relative standard deviation of (a) the electron resistances of single B impurities and (b) the hole resistances of single P impurities, as a function of the Si NW diameter  $d$  (same parameters as in Fig. 1). The inset in (b) is the resistance of individual P impurities in a  $\langle 111 \rangle$  Si NW with diameter  $d = 5$  nm (embedded in HfO<sub>2</sub>), as a function of their radial position. This particular Si NW is marked with an arrow in the main figure. The horizontal line and the shaded area in the inset are, respectively, the average resistance  $\langle R_{\text{imp}} \rangle$  and the  $\langle R_{\text{imp}} \rangle \pm \langle \Delta R_{\text{imp}}^2 \rangle^{1/2}$  interval.

structure again increase the average velocity of carriers and help suppress intersubband scattering. On the opposite, the topmost valence bands are almost twofold degenerate and heavy ( $m^* \simeq m_0$ ) in  $\langle 001 \rangle$  Si NWs, which explains the comparatively lower mobilities found for this orientation.

Fig. 1 also clearly emphasizes the importance of the gate dielectrics. While the mobility is not much limited by impurities in high- $\kappa$  gate oxides such as HfO<sub>2</sub>, and can even be enhanced in small Si NWs, it is far more degraded in SiO<sub>2</sub>. The impurities can really hinder the flow of electrons in ultimate  $\langle 111 \rangle$  and  $\langle 001 \rangle$  Si NWs, and the flow of holes in  $\langle 001 \rangle$  Si NWs embedded in SiO<sub>2</sub>. Indeed, the electrons and holes have little opportunities to bypass the impurities and must therefore tunnel through the barrier. At low energy, the transmission decreases exponentially (in a simple Wentzel-Kramers-Brillouin (WKB) approximation<sup>30</sup>) with the square root of the mass (part of the above orientational dependence), with the square root of the height of the barrier, and with its range. The latter are controlled by the gate oxide material and thickness, and possibly by the free carriers which screen the impurities. The thinner the oxide (i.e., the closer

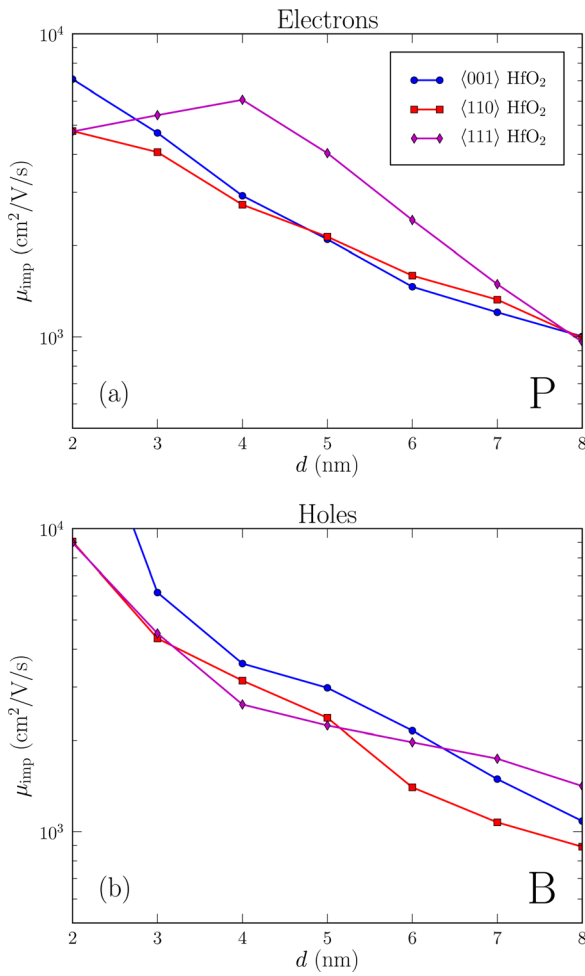


FIG. 3. Impurity-limited mobility of (a) electrons in P doped Si NWs and (b) holes in B doped Si NWs, as a function of diameter  $d$ , for different orientations. The NWs are surrounded by a 2 nm thick HfO<sub>2</sub> oxide and a metallic gate (gate-all-around geometry). The carrier density and impurity concentrations are  $n = n_{\text{imp}} = 10^{18} \text{ cm}^{-3}$ .

the gate), the faster the decrease of the impurity potential; and the larger its dielectric constant, the lower the barrier, especially close to the Si/oxide interface. The impurity-limited mobility is expected to increase with carrier density as the free electrons or holes will further reduce the height and range of the barrier, as discussed in Ref. 20. Such an increase of the mobility in the “ON” state might improve the switching performances (e.g.,  $I_{\text{ON}}/I_{\text{OFF}}$  ratio, subthreshold slope, etc) of Si NWs transistors.

The variability of ultimate devices is a major concern in microelectronics. Impurities are actually expected to be a major source of variability in Si NWs transistors. Not only the number of impurities can vary from one device to the other but also the resistance of each single impurity is dependent on its radial position in the NW. We have systematically investigated the statistics of individual impurity resistances in all NW orientations. The relative standard deviation  $\sigma_{\text{imp}} = \langle \Delta R_{\text{imp}}^2 \rangle^{1/2} / \langle R_{\text{imp}} \rangle$  of the impurity resistances is plotted in Fig. 2 as a function of NW diameter, orientation and gate oxide material, for minority carriers. As expected,  $\sigma_{\text{imp}}$  decreases with increasing NW diameter (for  $d > 5$  nm), and is slightly larger in HfO<sub>2</sub> than in SiO<sub>2</sub> (due to the enhanced screening of near-surface dopants). The

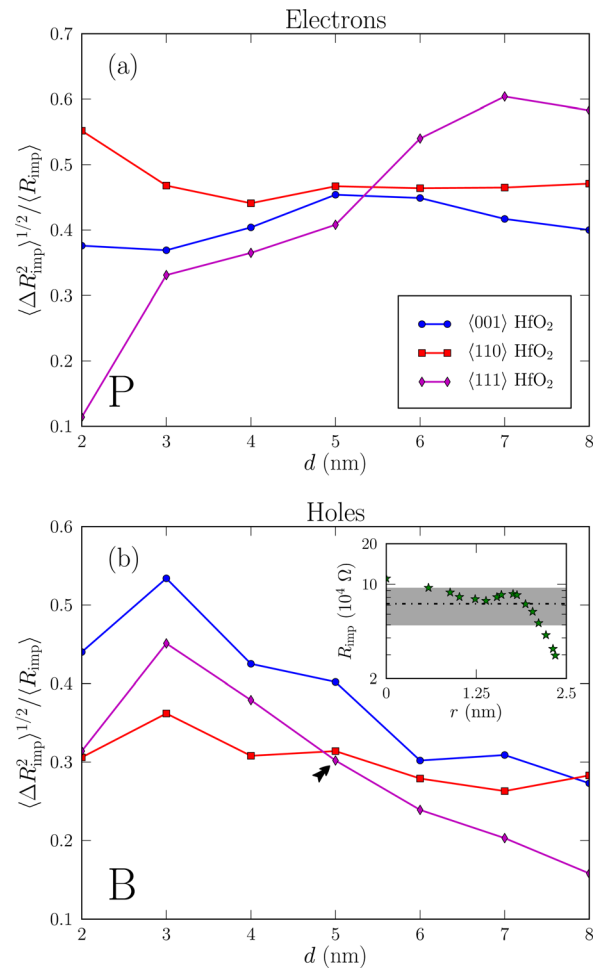


FIG. 4. Relative standard deviation of (a) the electron resistances of single P impurities and (b) the hole resistances of single B impurities, as a function of the Si NW diameter  $d$  (same parameters as in Fig. 3). The inset in (b) is the resistance of individual B impurities in a  $\langle 111 \rangle$  Si NW with diameter  $d = 5$  nm (embedded in HfO<sub>2</sub>), as a function of their radial position. This particular Si NW is marked with an arrow in the main figure. The horizontal line and the shaded area in the inset are the average resistance  $\langle R_{\text{imp}} \rangle$  and the  $\langle R_{\text{imp}} \rangle \pm \langle \Delta R_{\text{imp}}^2 \rangle^{1/2}$  standard deviation interval, respectively.

holes also show slightly less variability than the electrons, except in the least favorable  $\langle 100 \rangle$  orientation. The resistances of single impurities can span more than one order of magnitude from the center to the surface of the NW in the worst scenarios (see inset of Fig. 2(b)). These data pinpoint possible issues with the reproducibility of the characteristics of (even non-intentionally doped) ultimate NW devices.

We now discuss the impurity-limited mobility in the accumulation regime (transport of “majority” carriers, i.e., electrons in P-doped and holes in B-doped NWs). The mobility of electrons in P doped NWs and the mobility of holes in B doped NWs are plotted as a function of diameter  $d$  in Fig. 3 for the HfO<sub>2</sub> gate oxide. Interestingly, the mobility typically increases with decreasing  $d$ . The orientational dependence of the mobility is also much weaker and most often opposite to the inversion regime. Actually, the carriers now see the impurities as quantum wells. The transmission just above a quantum well embedded in a waveguide depends in a complex manner on its shape and does not necessarily increase when it gets thinner and shallow (that is, when the impurity is better screened), or when the mass of the carriers

decreases.<sup>31</sup> As a matter of fact, the same trends have been obtained for a SiO<sub>2</sub> gate oxide,<sup>20</sup> but with sometimes even larger mobilities. The coupling between the impurity well and the lateral confinement also gives rise to Fano resonances at the energies of the quasi-bound states of the higher subbands,<sup>16,20,31</sup> which can be responsible for a non-monotonous dependence of the impurity resistances on their radial position and on NW diameter.<sup>20</sup> The standard deviation of the single impurity resistances (Fig. 4) is actually smaller than for the minority carriers but shows more complex trends.

The above results suggest that there might be significant interactions between impurities as well as a complex interplay between impurity and phonon scattering (which is known to be strong in NWs (Refs. 12–14)). Phonons will indeed break phase coherence in multiple impurity scattering processes and mediate inelastic capture/release of carriers by the impurities.<sup>32,33</sup> This is, however, an open question which is beyond the scope of this paper.

To conclude, we have systematically investigated the impurity-limited electron and hole mobilities in gate-all-around Si NWs with different orientations and gate oxides. In the inversion regime, the  $\langle 110 \rangle$  and  $\langle 001 \rangle$  Si NWs show the best electron mobilities, while the  $\langle 110 \rangle$  and  $\langle 111 \rangle$  Si NWs show the best hole mobilities, as expected from simple band structure arguments. Achieving large minority carriers mobility however calls for high- $\kappa$  oxides which can efficiently screen the barriers introduced by the impurities. The variability of single impurity resistances in small NWs is very significant in the sub-10 nm regime, whatever the orientation. The mobility of majority carriers is found to increase with decreasing NW diameter as a result of the complex interplay between the lateral confinement and the impurity well.

This work was supported by the French National Research Agency (ANR) projects QUASANOVA and SIMPSSON. The calculations were run at the GENCI-CCRT and GENCI-CINES supercomputing centers.

<sup>1</sup>J.-P. Colinge, *Solid-State Electron.* **48**, 897 (2004).

<sup>2</sup>N. Singh, A. Agarwal, L. Bera, T. Liow, R. Yang, S. Rustagi, C. Tung, R. Kumar, G. Lo, N. Balasubramanian, and D.-L. Kwong, *IEEE Electron Device Lett.* **27**, 383 (2006).

<sup>3</sup>S. Rustagi, N. Singh, Y. Lim, G. Zhang, S. Wang, G. Lo, N. Balasubramanian, and D.-L. Kwong, *IEEE Electron Device Lett.* **28**, 909 (2007).

<sup>4</sup>K. H. Cho, K. H. Yeo, Y. Y. Yeoh, S. D. Suk, M. Li, J. M. Lee, M.-S. Kim, D.-W. Kim, D. Park, B. H. Hong, Y. C. Jung, and S. W. Hwang, *Appl. Phys. Lett.* **92**, 052102 (2008).

<sup>5</sup>J. Martinez, R. V. Martnez, and R. Garcia, *Nano Lett.* **8**, 3636 (2008).

<sup>6</sup>T. Hiramoto, J. Chen, and T. Saraya, in *10th IEEE International Conference on Solid-State and Integrated Circuit Technology (ICSICT)*, edited by T.-A. Tang and Y.-L. Jiang, (IEEE, 2010), pp. 9–12.

<sup>7</sup>K. Trivedi, H. Yuk, H. C. Floresca, M. J. Kim, and W. Hu, *Nano Lett.* **11**, 1412 (2011).

<sup>8</sup>M. V. Fernández-Serra, C. Adessi, and X. Blase, *Phys. Rev. Lett.* **96**, 166805 (2006).

<sup>9</sup>M.-V. Fernández-Serra, C. Adessi, and X. Blase, *Nano Lett.* **6**, 2674 (2006).

<sup>10</sup>T. Markussen, R. Rurali, M. Brandbyge, and A.-P. Jauho, *Phys. Rev. B* **74**, 245313 (2006).

<sup>11</sup>T. Markussen, R. Rurali, A.-P. Jauho, and M. Brandbyge, *Phys. Rev. Lett.* **99**, 076803 (2007).

<sup>12</sup>M. Luisier and G. Klimeck, *Phys. Rev. B* **80**, 155430 (2009).

<sup>13</sup>W. Zhang, C. Delerue, Y.-M. Niquet, G. Allan, and E. Wang, *Phys. Rev. B* **82**, 115319 (2010).

<sup>14</sup>M. Luisier, *Appl. Phys. Lett.* **98**, 032111 (2011).

<sup>15</sup>J. H. Oh, D. Ahn, Y. S. Yu, and S. W. Hwang, *Phys. Rev. B* **77**, 035313 (2008).

<sup>16</sup>R. Rurali, T. Markussen, J. Suñé, M. Brandbyge, and A.-P. Jauho, *Nano Lett.* **8**, 2825 (2008).

<sup>17</sup>A. Martinez, A. R. Brown, N. Seoane, and A. Asenov, *J. Phys.: Conf. Ser.* **193**, 012047 (2009).

<sup>18</sup>M. Bescond, M. Lannoo, F. Michelini, L. Raymond, and M. G. Pala, *Microelectron. J.* **40**, 756 (2009).

<sup>19</sup>M. Bescond, M. Lannoo, L. Raymond, and F. Michelini, *J. Appl. Phys.* **107**, 093703 (2010).

<sup>20</sup>M. P. Persson, H. Mera, Y.-M. Niquet, C. Delerue, and M. Diarra, *Phys. Rev. B* **82**, 115318 (2010).

<sup>21</sup>N. Pons, N. Cavassilas, L. Raymond, F. Michelini, M. Lannoo, and M. Bescond, *Appl. Phys. Lett.* **99**, 082113 (2011).

<sup>22</sup>T. B. Boykin, G. Klimeck, and F. Oyafuso, *Phys. Rev. B* **69**, 115201 (2004).

<sup>23</sup>Y. M. Niquet, A. Lherbier, N. H. Quang, M. V. Fernández-Serra, X. Blase, and C. Delerue, *Phys. Rev. B* **73**, 165319 (2006).

<sup>24</sup>M. Diarra, Y.-M. Niquet, C. Delerue, and G. Allan, *Phys. Rev. B* **75**, 045301 (2007).

<sup>25</sup>R. Landauer, *IBM J. Res. Dev.* **1**, 223 (1957).

<sup>26</sup>M. Büttiker and R. Landauer, *Phys. Rev. Lett.* **49**, 1739 (1982).

<sup>27</sup>K. Kazymyrenko and X. Waintal, *Phys. Rev. B* **77**, 115119 (2008).

<sup>28</sup>The mobility simply scales as  $1/n_{\text{imp}}$  for a given  $n$ . Note that in the bulk limit ( $d \rightarrow \infty$ ), where  $\mu_{\text{imp}}$  is independent of diameter, the resistance  $\langle R_{\text{imp}} \rangle$  of single impurities is expected to decrease as  $1/d^4$ .

<sup>29</sup>M. P. Persson, A. Lherbier, Y.-M. Niquet, F. Triozon, and S. Roche, *Nano Lett.* **8**, 4146 (2008).

<sup>30</sup>A. Messiah, *Quantum Mechanics* (Elsevier, 1961).

<sup>31</sup>V. Vargiamidis and H. M. Polatoglou, *Phys. Rev. B* **72**, 195333 (2005).

<sup>32</sup>W. Cai, P. Hu, T. F. Zheng, B. Yudanin, and M. Lax, *Phys. Rev. B* **41**, 3513 (1990).

<sup>33</sup>V. Kagan, *Phys. Solid State* **47**, 217 (2005).